

A NEW FLYBACK-CURRENT-FED PUSH-PULL DC-DC CONVERTER

Domingo A. Ruiz-Caballero and Ivo Barbi

Federal University of Santa Catarina

Department of Electrical Engineering

Power Electronics Institute

P. O. Box: 5119 88.040-970 - Florianópolis - SC - Brazil.

E-mail: domingo@inep.ufsc.br

ABSTRACT - This paper introduces a new flyback-current-fed push-pull dc-dc converter whose significant advantages in comparison with the conventional one are: reduction in the number of output diodes and unified output characteristics to represent both the buck and the boost operation modes in the continuous conduction mode. Theoretical analysis, design methodology, and experimental results taken from a 600W, 25kHz laboratory prototype are presented in this paper. The circuit introduced is suitable for switching mode power supply design and power factor correction applications as well.

NOMENCLATURE

\bar{I}_O	Normalized Output Current.
\bar{V}_O	Normalized Output Voltage.
N	Transformers Turns-Ratio.
$\bar{I}_{L_{1Pmin}}$	Normalized minimum Current Through the Primary Winding L_{1P} .
$\bar{I}_{L_{1Pmax}}$	Normalized maximum Current Through the Primary Winding L_{1P} .
$\bar{I}_{L_{1Smin}}$	Normalized minimum Current Through the Primary Winding L_{1S} .
$\bar{I}_{L_{1Smax}}$	Normalized maximum Current Through the Primary Winding L_{1S} .
$\bar{\Delta i}_{L_{1S}}$	Normalized Ripple Current Through the Secondary Winding L_{1S} .
$\bar{\Delta i}_{L_{1P}}$	Normalized Ripple Current Through the Primary Winding L_{1P} .
V_{GS}	Gate-source Mosfet Voltage.
$I_{L_{1P}}$	Current Through the Primary Winding L_{1P} .
$I_{L_{1S}}$	Current Through the Secondary Winding L_{1S} .
$V_{L_{2P}}$	Voltage across the Push-Pull Primary Winding L_{2P} .
η	Efficiency.
I_i	Average Input Current.
I_o	Average Output Current.
V_o	Output Voltage.
V_i	Input Voltage.
D	Duty-Ratio.
V_{S1}, V_{S2}	Voltage across Switches S_1 and S_2 .
i_{S1}, i_{S2}	Current through Switches S_1 and S_2 .
F_s	Switching Frequency.
t	Time.
Δt_1	Time interval where for both buck and boost modes S_1 is turn-on.

Δt_1 Time interval where for both buck and boost modes a current flows through the flyback transformer.

I. INTRODUCTION

The flyback-current-fed push-pull dc-dc converter[1] [2], has several advantages over the conventional voltage or current-fed push-pull ones. It has one single input and no output inductor, which makes it a good choice for a multiple output power supply. Besides, it provides inherent protection against transformer saturation. It is also recognized that the mentioned converter is more reliable than the conventional push-pull one due to the presence of the input inductor.

However, some disadvantages have been detected, namely, the existence of four diodes on the secondary side, and the impossibility of representing the operation for duty-ratio from zero up to one, by the same set of output characteristics.

The circuit introduced in this paper is generated from the traditional flyback-current-fed push-pull topology, simply by removing the push-pull diodes.

The new converter is composed by a push-pull transformer and two inductors (input and output) magnetically coupled, that form the flyback transformer. In addition, the circuit includes two switches and two output diodes. The converter's characteristics are as follows:

a) it has two operation modes namely buck and boost, that depend exclusively on the duty-ratio. For duty-ratio less than 0.5, it operates in the buck mode (non-overlapping mode) and for duty-ratio larger than 0.5, it operates in the boost mode (overlapping mode).

b) its switches are at the same reference point, which simplifies the driving circuitry.

c) when both transformers have the same turns ratio, the output characteristics in continuous conduction mode are the same for both the overlapping and the non-overlapping operation modes.

d) it has only two output diodes.

The operation of the new circuit is described in the following section.

II. PRINCIPLE OF OPERATION FOR $D < 0.5$.

In the buck mode, four topological states exist within a switching period. However, it is necessary to describe only two of them, as the remaining two stages are analogous.

The stages of operation for a half-cycle are shown in Fig. 1. They are described as follows:

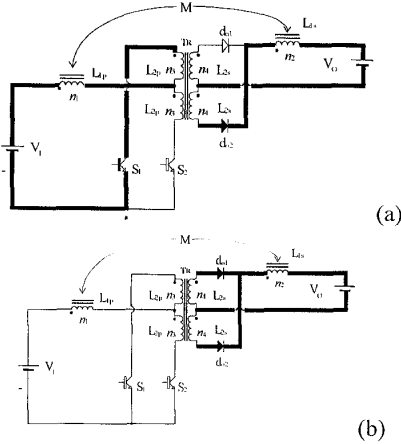


Fig. 1 - First (a) and second (b) stages for $D < 0.5$.

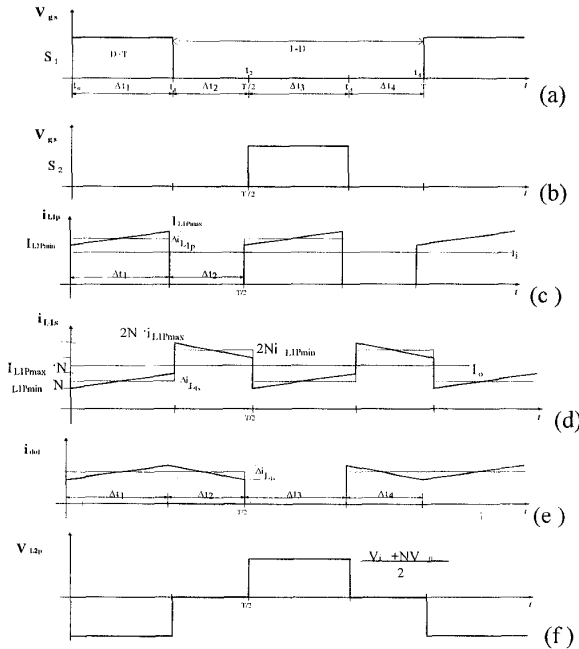


Fig. 2 - Waveforms for the new converter working at $D < 0.5$ in CCM: a) and b) driving signals, c) input current, d) current through the inductor L_{1s} , e) current through the output diodes, and f) voltage across the primary winding of the push pull transformer.

First stage (t_0, t_1): at the instant $t=t_0$, S_1 turns on, a current flows through L_{1p} , L_{2p} and S_1 . The voltage across L_{2p} is reflected across the push-pull secondary windings (L_{2s}), and d_{o2} is turned on. The flyback transformer acts as an inductor, storing energy. The load receives energy only from the push-pull transformer. This stage exists for both the continuous and the discontinuous conduction modes.

Second stage (t_1, t_2): at $t=t_1$, S_1 turns off and the flyback transformer transfers energy to the load with a current which is twice the current of the previous time interval. The value of the current flowing through each diode is equal to the current through the diode that was on during

the previous time interval. Since both diodes are conducting, the push-pull transformer is short-circuited. This stage ends when S_2 turns on. In the discontinuous conduction mode this stage ends when the inductor current reaches zero and then a third stage can be observed, in which there is no transfer of energy. The load is supplied by the output capacitor.

The corresponding theoretical waveforms for continuous and discontinuous current mode is shown in Figures 2 and 3, respectively.

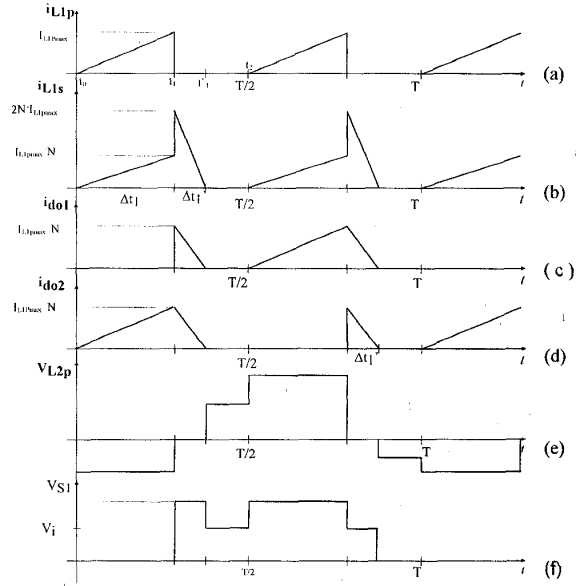


Fig. 3 - Waveforms for discontinuous operation mode at $D < 0.5$: a) current through the primary winding L_{1p} , b) current through secondary winding L_{1s} , c) and d) current through output diodes, e) voltage across the primary winding of the push pull transformer, and f) voltage across the switches.

III. PRINCIPLE OF OPERATION FOR $D > 0.5$.

The circuits representing the stages of operation for a half cycle are shown in Fig. 4.

First stage (t_0, t_1): when this stage begins, switch S_2 is already on. At $t=t_0$, S_1 is gated on, conducting simultaneously with S_2 . Current starts flowing through the push-pull primary windings L_{2p} so that the fluxes induced by the primary windings are in opposite directions, causing a magnetic short-circuit in the transformer. As a result energy is stored in L_{1p} .

Second stage (t_1, t_2): at the instant $t=t_1$, S_2 is turned off and energy begins to be transferred to the load. This energy transfer occurs in two ways: directly through the push-pull transformer and indirectly through the flyback transformer (which delivers the energy stored during the previous time interval). When operating in the discontinuous mode, the boost mode also presents a third stage, with no energy transfer, in which the load is supplied by the output capacitor.

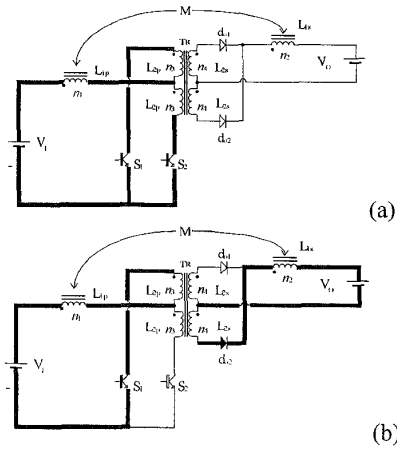


Fig. 4 -First (a) and second (b) stages for $D>0.5$.

For the discontinuous conduction mode, a third stage starts when the current through the flyback transformer primary winding becomes zero. There is no energy transfer in this interval, which finish at $t=T/2$, when S_2 turns on.

The theoretical waveforms for CCM and DCM are shown in Figs. 5 and 6, respectively.

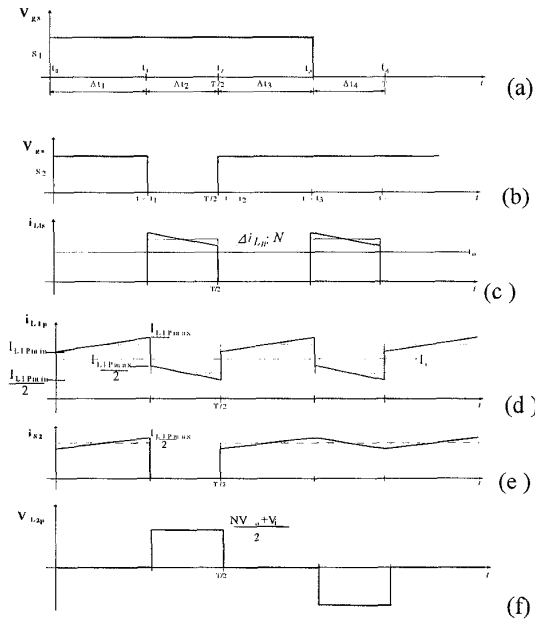


Fig.5- Waveforms for the converter operating at $D>0.5$ in CCM: a) and b) driving signals of S_1 and S_2 , c) current through the secondary winding L_{1s} , d) current through the primary winding L_{1p} , e) current through the switches, and f) voltage across the primary winding of the push-pull transformer.

IV. OUTPUT CHARACTERISTICS

The output characteristics in the continuous current mode for any duty-ratio are given by (1).

$$\bar{V}_o = \frac{D}{(1-D)} \quad (1)$$



Fig. 6.- Waveforms for the discontinuous conduction mode and $D>0.5$: a) current through the primary winding L_{1p} , b) current through secondary winding L_{1s} , c) current through switch S_1 , d) current through switch S_2 , e) voltage across the primary winding of the push-pull transformer L_{2p} , and f) voltage across the switches.

In DCM the output characteristics are represented by two different expressions. For the buck mode, they are given by (2).

$$\bar{V}_o = \frac{D^2}{(2 \cdot \bar{I}_o + D^2)} \quad (2)$$

The boundary between DCM and CCM for $D<0.5$ is given by (3).

$$\bar{V}_o = \frac{1 - 4 \cdot \bar{I}_o - \sqrt{1 - 16 \cdot \bar{I}_o}}{2 \cdot (2 \cdot \bar{I}_o + 1)} \quad (3)$$

For the boost mode, the output characteristics in DCM are given by (4).

$$\bar{V}_o = \frac{(2 \cdot D - 1)^2 + 2 \cdot \bar{I}_o}{2 \cdot \bar{I}_o} \quad (4)$$

The boundary between DCM and CCM for $D>0.5$ is given by (5).

$$\bar{I}_o = \frac{[\bar{V}_o - 1]}{2 \cdot [1 + \bar{V}_o]^2} \quad (5)$$

The normalized load current is given by (6).

$$\bar{I}_o = \frac{2 \cdot L_{1s} \cdot F_S \cdot N}{V_i} \cdot I_o \quad (6)$$

The normalized load voltage is given by (7).

$$\bar{V}_o = N \cdot \frac{V_o}{V_i} \quad (7)$$

The transformers turns-ratio are given by (8).

$$N = \frac{n_1}{n_2} = \frac{n_3}{n_4} \quad (8)$$

The unified output characteristics of the converter are shown in Fig. 7. They are composed by the superposition of the individual output characteristics of the classic buck and boost converters.

For $D=0.5$ the converter will never operate in the discontinuous conduction mode, even for light loads.

The minimal current load which ensures continuous current mode is $\bar{I}_{o\min} = 0.0625$ for both the buck and the boost modes.

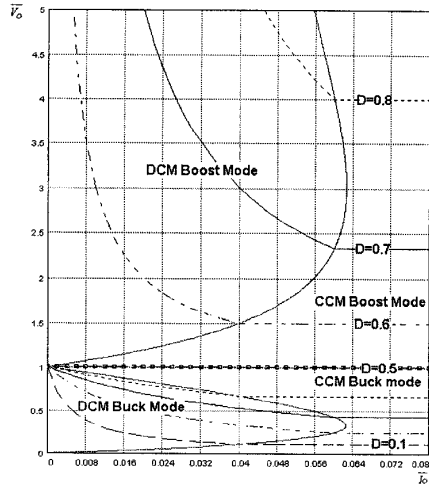


Fig. 7- Unified output characteristics.

V. INPUT AND OUTPUT CURRENT RIPPLE.

For $D < 0.5$, according to the waveforms shown in Fig. 2, the normalized output current ripple is given by (9)

$$\bar{\Delta i}_{L_{IS}} = \bar{I}_{L_{IS\max}} - \bar{I}_{L_{IS\min}} \quad (9)$$

$\bar{I}_{L_{IS\max}}$ and $\bar{I}_{L_{IS\min}}$ are given by (10) and (11), respectively.

$$\bar{I}_{L_{IS\max}} = \frac{\bar{I}_o}{(1-D)} + \frac{D \cdot (1-2 \cdot D)}{4 \cdot (1-D)} \quad (10)$$

$$\bar{I}_{L_{IS\min}} = \frac{\bar{I}_o}{(1-D)} - \frac{D \cdot (1-2 \cdot D)}{4 \cdot (1-D)} \quad (11)$$

By substituting (10) and (11) into (9), one obtains (12).

$$\bar{\Delta i}_{L_{IS}} = \frac{(1-2 \cdot D) \cdot D}{2 \cdot (1-D)} \quad (12)$$

The current $\bar{\Delta i}_{L_{IS}}$ is defined by (13).

$$\bar{\Delta i}_{L_{IS}} = \frac{2 \cdot L_{IS} \cdot F_S \cdot N}{V_i} \cdot \Delta i_{L_{IS}} \quad (13)$$

For $D > 0.5$, according to the waveforms shown in Fig. 5, the normalized input current ripple is given by (14).

$$\bar{\Delta i}_{L_{IP}} = \bar{I}_{L_{IP\max}} - \bar{I}_{L_{IP\min}} \quad (14)$$

$\bar{I}_{L_{IP\max}}$ and $\bar{I}_{L_{IP\min}}$ are given by (15) and (16) respectively.

$$\bar{I}_{L_{IP\max}} = \frac{\bar{I}_i}{D} + \frac{(2 \cdot D - 1) \cdot (1 - D)}{2 \cdot D} \quad (15)$$

$$\bar{I}_{L_{IP\min}} = \frac{\bar{I}_i}{D} - \frac{(2 \cdot D - 1) \cdot (1 - D)}{2 \cdot D} \quad (16)$$

By substituting (15) and (16) into (14), one obtains (17).

$$\bar{\Delta i}_{L_{IP}} = \frac{(2 \cdot D - 1) \cdot (1 - D)}{D} \quad (17)$$

The current $\bar{\Delta i}_{L_{IP}}$ is defined by (18).

$$\bar{\Delta i}_{L_{IP}} = \frac{2 \cdot L_{IP} \cdot F_S \cdot N}{V_o} \cdot \Delta i_{L_{IP}} \quad (18)$$

Expressions (12) and (17) are represented in Fig. 8a and Fig. 8b respectively.

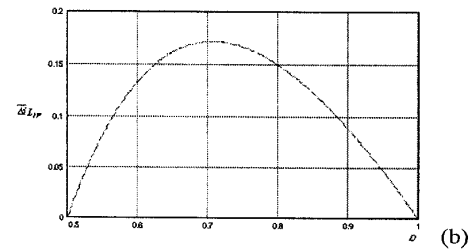
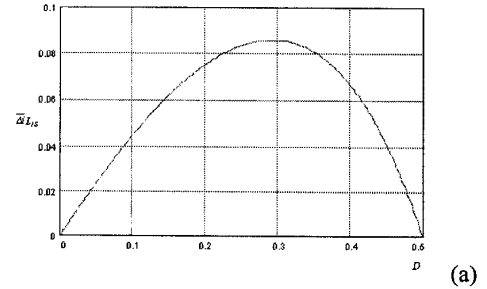


Fig. 8- Current ripple for (a) buck and (b) boost modes as function of D.

The current ripples $\overline{\Delta i}_{L_{1P}}$ and $\overline{\Delta i}_{L_{1S}}$ are similar to the primary and secondary flyback transformer current ripple of the conventional push-pull converter.

They become theoretically equal to zero when L_{1P} and L_{1S} are very large. In this case, the output current for $D < 0.5$, and the input current for $D > 0.5$, have two levels different from zero, as shown in Figures 9a and 9b. In the particular case when $D = 0.5$, both input and output current are ripple-free.

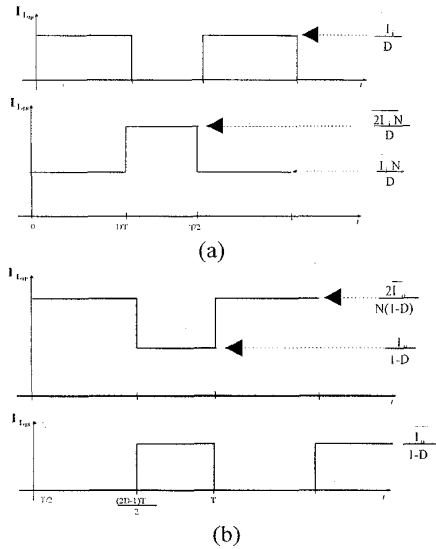


Fig. 9- Input and output currents for (a) $D < 0.5$ and (b) $D > 0.5$, with $L_{1P} = L_{1S} = \infty$ and $N_1 = N_2$.

The variations observed in $I_{L_{1S}}$ (Fig 9a) and $I_{L_{1P}}$ (Fig 9b) are a consequence of the instantaneous flux preservation of the flyback transformer for a period of operation.

VI - EXPERIMENTAL RESULTS

A laboratory prototype, operating in the continuous conduction mode, has been designed and implemented. Its specifications are as follows:

$$P_o = 600W, \quad V_{i_{max}} = 48V, \quad V_{i_{min}} = 15V, \quad F_S = 25kHz,$$

$$V_o = 60V, \quad I_o = 10A, \quad \frac{\Delta V_{CO}}{V_o} = 0.01, \quad \Delta V_{SW} = 1V$$

$$\Delta i_2 = 0.1 \cdot I_o = 1A,$$

The turns ratio N is calculated by using $D = 0.3$, which is the duty-ratio that causes the maximum output current ripple in the buck mode. With the saturation voltage across the switches equal to 1V, from (1), we obtain $N = 0.33$.

The primary and secondary flyback transformer inductances L_{1P} and L_{1S} are calculated. The obtained values are $L_{1S} = 249.312 \mu H$ and $L_{1P} = 27.15 \mu H$.

The duty-ratio for $V_{i_{min}}$ and $V_{i_{max}}$, calculated using (1) are as follows:

$$D_{min} = 0.3 \quad \text{for} \quad V_{i_{max}} = 48V, \quad \text{and} \quad D_{max} = 0.6 \quad \text{for} \quad V_{i_{min}} = 15V.$$

The power and control diagrams are shown in Fig. 10 and the parameters of the prototype are given in Table I and Table II for the control circuit and the power stage, respectively.

Table I - Control Circuit Components.

P1	56 k Ω
P2, P3,	1 k Ω
P4	10 k Ω
R ₁ , R ₂	5.6 k Ω , 1/8W
R ₃ , R ₄	15 k Ω , 1/8W
R ₅ , R ₆	100 Ω , 1/8W
R ₇ , R ₈	1 k Ω , 1/8W
R ₉ , R ₁₀	15 k Ω , 1/4W
R ₁₁ , R ₁₂	1 k Ω , 1/4W
R ₁₃ , R ₁₄	15 k Ω , 1/4W
R ₁₅ , R ₁₆ , R ₁₇ , R ₁₈	1 k Ω , 1/4W
R ₁₉ , R ₂₀	2.2 k Ω , 1/4W
R ₂₁ , R ₂₂	6.8 Ω , 1/4W
R ₂₃	20 k Ω , 1/4W
C ₁	82 pF
C ₂	100 nF
C ₃ , C ₄	27 pF
C ₅ , C ₆ , C ₇	56 nF
C ₈ , C ₉	100 nF
C ₁₀ , C ₁₁	1 nF
C ₁₂	1.2 nF
d ₁ , d ₂ , d ₃ , d ₄ , d ₅ , d ₆	1N4148
dz ₁ , dz ₂	2.7V 1N4371
dz ₃ , dz ₄	5.1V 1N751
Q ₁ , Q ₂	BC558B, PNP
Q ₃ , Q ₄	BC537, NPN
Q ₅ , Q ₆ , Q ₇ , Q ₈ , Q ₉ , Q ₁₀	BC327, PNP
C ₁ , I ₁	LM311
C ₁ , I ₂	CD4047BE
C ₁ , I ₃	CD4528BE

Table II - Power Stage Components.

S ₁ , S ₂	MOSFET IRFP150
do ₁ , do ₂	MUR 135
dg ₁ , dg ₂	SKE 4t2/04, Semikron
Cg ₁ , Cg ₂	4700pF, 1.6kV polypropylene
Rg ₁ , Rg ₂	47k Ω , 1/2W
Co	1000uF, 250V
Cgs	100uF
ds ₁ , ds ₂	MUR 1530
Rgs	60 Ω
T _{FL} : core E-65/26, N=0.33 airgap: 0.5mm.	n ₁ =9 turns, AWG 22, 13 wires. n ₂ =27 turns, AWG 22, 8 wires.
T _{pp} : core E-65/26, N=0.33	n ₃ =n ₅ =6 turns, AWG 22, 9 wires. n ₄ =n ₆ =18 turns, AWG 22, 5 wires.

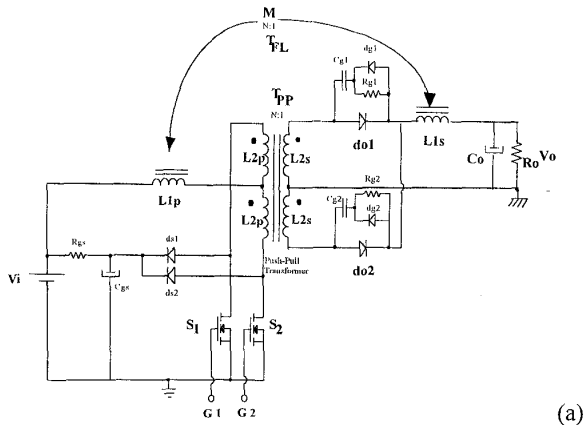


Fig. 10 -Power (a) and control (b) diagram.

Figure 11a shows the input (I_{L1P}) and the output currents (I_{L1S}) for $D=0.3$ at rated load power, which is equal to 600W. Fig. 11b shows the input (I_{L1P}) and the output current (I_{L1S}) for $D=0.6$. Finally, Fig. 11c shows the input (I_{L1P}) and the output currents (I_{L1S}) for $D=0.5$. The waveforms shown in Figures 11b and 11c were taken at output power equal to 300W.

The experimental waveforms confirm that for $D=0.5$, both the output and the input currents are ripple-free, which characterizes the behavior of an ideal DC-DC transformer.

Figure 12 shows the experimentally obtained efficiency of the implemented converter, utilizing a dissipative clamping circuit for $V_o=60V$ and $V_i=48V$.

VII. CONCLUSIONS

From our study as reported in this paper, we draw the following conclusions:

- The new converter preserves all the basic properties of the conventional flyback current-fed push-pull converter with fewer components.
- It operates in both buck and boost modes which are represented by the same mathematical model.
- It presents high efficiency, which can be improved with the utilization of regenerative clamping.

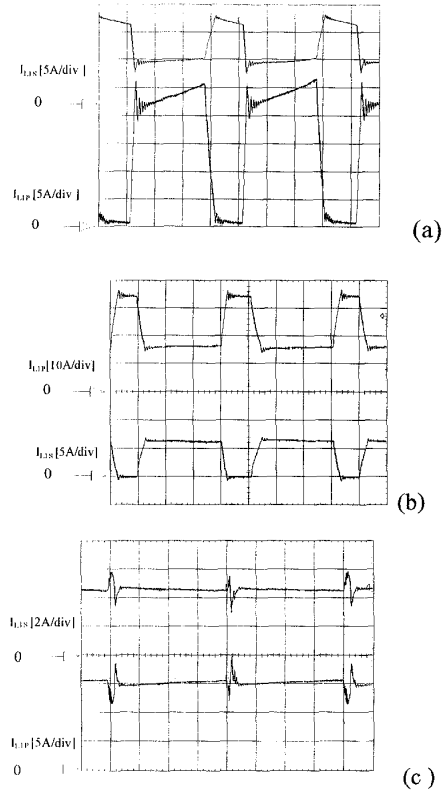


Fig. 11- Experimentally obtained input (I_{L1P}) and output (I_{L1S}) currents for (a) $D=0.3$, (b) $D=0.6$, (c) $D=0.5$, with $5 \mu \text{ sec/div}$.

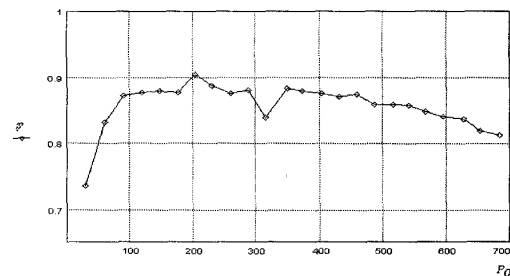


Fig. 12 - Obtained efficiency as a function of the converter output power in the buck mode.

VIII. REFERENCES

- [1] V.J. Thottuvelil, T.G. Wilson and H.A. Owen, Jr., "Analysis and Design of a Push-Pull Current-Fed Converter", IEEE Power Electronic Specialist Conference, 1981 Record, pp. 192-203.
- [2] R. Redl and N. Sokal, "Push-Pull Current-Fed, Multiple output Regulated Wide Input Range DC/DC Power Converter with only one Inductor and With 0 to 100% Switch Duty Ratio: Operation at Duty Ratio Below 50 %", IEEE Power Electronic Specialist Conference, 1981 Record, pp. 204-212.